Jurnal Teknik Sipil & Perencanaan 25 (1) (2023) p 34 - 51

JURNAL TEKNIK SIPIL & PERENCANAAN

10.15294/jtsp.v25i1.42954

The behavior of Axial Bearing Pile under Liquefaction Condition Based on Empirical and 3D Numerical Simulation

Ali Zakariya[1, 2, a)], Ahmad Rifa'i[1, b)], and Sito Ismanti[1, c)]

[1]*Department of Civil and Environmental Engineering, Universitas Gadjah Mada, Sleman, Indonesia, 55281.*
[2]*Directorate General of Highways, Ministry of Public Works and Housing, Jakarta, Indonesia, 12110.*

[a)] ali.zakariya@pu.go.id
[b)] Corresponding author: ahmad.rifai@ugm.ac.id
[c)] sito.ismanti@ugm.ac.id

Abstract. The liquefaction phenomenon affects to bearing capacity losses of building foundations. When liquefaction occurs in loose sandy soils, the pore water pressure increases, and the effective soil stress decreases significantly. This study deals with the bored pile foundation of the Kretek 2 bridge, which is in an area with high vulnerability to liquefaction. The study aimed to estimate the axial load-bearing capacity of the foundation of the Kretek 2 bridge under liquefaction conditions. This study compares the results of calculations using empirical approaches with 3D numerical simulation modeling using MIDAS GTS NX. The results of the empirical calculations show a reduction in the axial bearing capacity of the foundation under liquefaction conditions of 2.88-8.16% and 2.63-7.23% for the approach of Reese and Wright 1977 and O'Neill and Reese 1989, respectively. While using 3D numerical modeling, although there was a decrease in skin resistance, there was no significant decrease in the total bearing capacity, and it was still above the design load (3632.56>3456.02 kN). Based on these results, the bearing capacity of the installed Kretek 2 Bridge foundation is still capable of receiving loads during static and liquefaction states.

Keywords: bearing capacity losses, bored pile foundation, 3D numerical simulation, MIDAS GTS NX, skin resistance

INTRODUCTION

After Niigata Earthquake in 1964, many infrastructures collapsed due to liquefaction, such as the Apartment Building and Showa Bridge. Liquefaction is a phenomenon that occurs when soil becomes liquified due to strong earthquakes, loose sandy soil, and shallow groundwater level, and it can affect soil-bearing capacity losses (see Figure 1. a). According to Byrne et al (2006), During the Niigata earthquake, liquefaction caused apartment buildings losses of their foundation supports, then overturn or sink (see Figure 1. b) [1]. Another researcher, Dash et al (2010), stated that the Showa Bridge collapsed due to lateral loads and additional free-standing piles when the top soil layer experienced liquified, creating a large moment so that the piles on the pier experienced buckling failure [2]. The liquefaction phenomenon causes the length of the free-standing pile to increase in the liquefied soil layer. As a result, the structure can fail with the dynamic amplification mechanism.

In 2021, The Directorate General of Highways (DJBM), Ministry of Public Works and Housing (PUPR), issued Guidelines number: 02/M/BM/2021 concerning Practical Guidelines for Bridge Technical Planning 2021 [3], which requires that each design of standard bridge in Indonesia with consideration the potential for liquefaction and its impact

on bridges. Bridge over high liquefaction potential conditions, the skin resistance in soil layers should ignore. Shallow foundations are not recommended to be applied, except soil improvement techniques are applied to eliminate liquefaction potential. Therefore, designing and constructing infrastructures in high-susceptibility liquefaction areas must consider the liquefaction effect on the foundation.

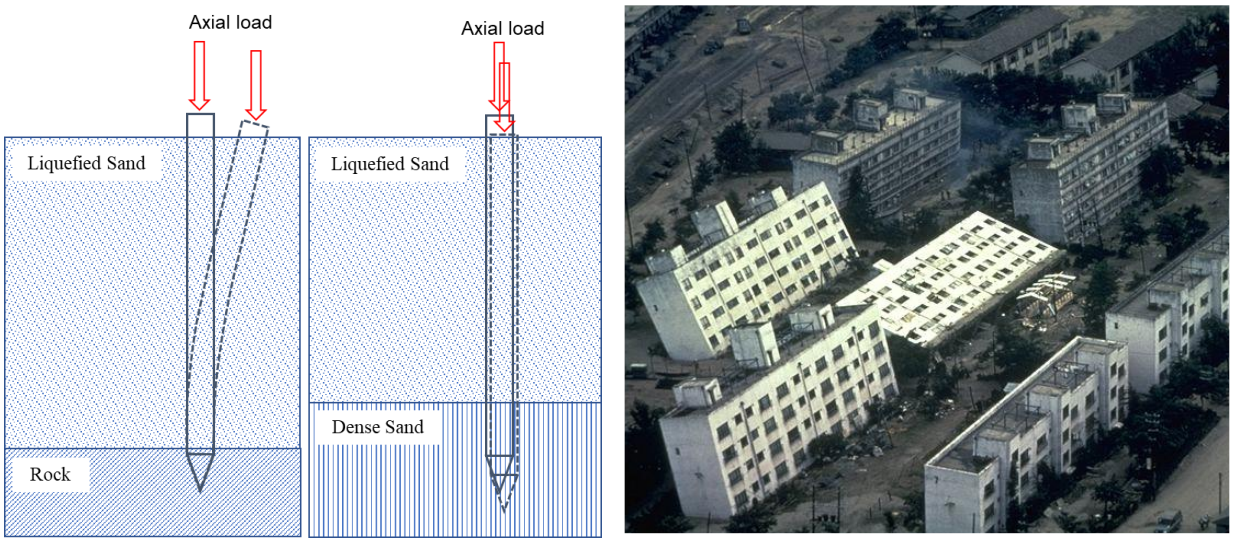

(a) (b)

FIGURE 1. (a) Single pile failure mechanism due to soil liquefaction; end bearing pile (on the left), and friction pile (on the right) (Madabhusi et al 2009) [4], (b) Apartment building collapse after 1964 Niigata earthquake (Byrne et al 2006)

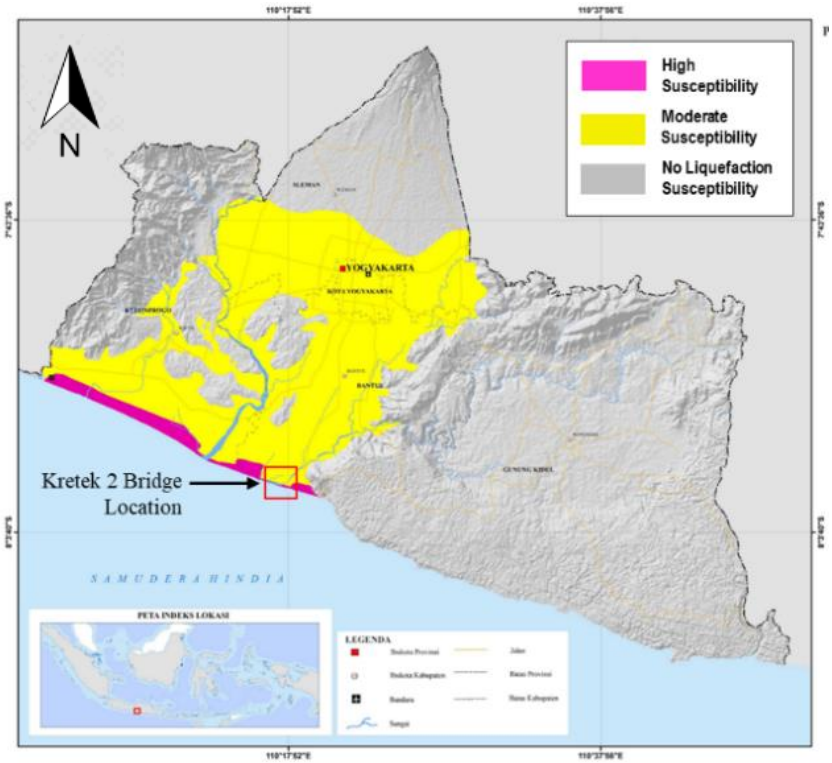

FIGURE 2. Liquefaction susceptibility zone map on Special Region of Yogyakarta (Badan Geology, 2019 with modification [5])

MATERIAL AND METHOD

Research Location

This study examines the foundation of the Kretek 2 Bridge against the liquefaction potential due to the bridge located over the liquefaction susceptibility area (see Figure 2). The Kretek 2 Bridge is located in Bantul Regency, Yogyakarta Special Region, Indonesia. Its location area has high liquefaction susceptibility due to shallow water tables, cohesionless soil types, and strong seismic sources. According to Muntafi et al (2020), in a case study of the 2006 Yogyakarta earthquake, the closer a building is to the epicenter, the higher the damage value [6]. In previous research, Sari (2017) designed the Kretek 2 bridge. Yet, the design differs from the built bridge [7]. Thus, the foundation of the Kretek 2 bridge must be recalculated to estimate the axial bearing and liquefaction effect on the foundation.

Bridge Load

Before calculating the length and amount of pile foundation, the working load on the foundation must be known first. In the regulation of SNI 1725:2016 [8], the combination of loads in the section becomes an ultimate combination to determine the ultimate limit, a service combination to determine the service limit, an extreme combination to determine the extreme limit of the condition or ship collision, flooding or other hydraulic loads, and a fatigue combination to determine the limit fatigue from a load of repetitions. In this study, the load output is used from previous research (Zakariya et al, 2022) [9], the load output of each abutment/pier is as follows:

TABLE 1. Load design from the upper structure

Abutment/ Pier	Pile Diameter (m)	Pile Total (unit)	Pile Length (m)	Load Design (kN)
P1	1	19	32.0	44577.00
P2	1	21	32.0	56752.00
P3	1	21	32.0	56752.00
P4	1	21	32.0	56752.00
P5	1	21	32.0	56752.00
P6	1	24	34.0	56752.00
P7	1	24	34.0	56752.00
P8	1	27	34.0	64559.28
A2	1	14	34.0	44577.00

Pile Bearing Capacity

The axial bearing capacity of a pile foundation can be calculated by estimating the skin resistance and the end bearing of the pile. According to Hardiyatmo (2018) [10], the pile-bearing capacity can be calculated using the following formula:

$$Q_u = Q_b + Q_s - W_P \quad (1)$$

where Q_u is ultimate bearing capacity, Q_b is the end-bearing capacity, Q_s is skin resistance capacity, W_P is pile weight. When estimating values of Q_b and Q_s, it is determined by the type of soil, the shape of the pile, the kind of pile construction, and the depth of the pile. The methods commonly used for sandy soils in Indonesia are those of Meyerhof (1976) [11], Reese and Wright (1977) [12], and O'Neill and Reese (1989) [13] method. For clayey soils, this study used Reese et al (1977) [14]. Some of these researchers conducted an empirical relationship between the value of SPT-N with the ultimate tip bearing and skin resistance. This study uses SPT-N soil survey data and soil properties as a reference for bearing capacity calculations.

Reese and Wright (1977) Method for Sandy Soil

The bearing capacity of the bored pile foundation can be calculated using Reese and Wright's (1977) method from the sum of end bearing and skin resistance minus the dead weight of the bored pile. The following equation determines the ultimate bearing capacity of the bored pile:

$$Q_b = A_b f_b \tag{2}$$

$$f_b = \frac{2}{3} N_{SPT}(tsf) \text{ for } N_{SPT} \leq 60 \tag{3}$$

$$f_b = 40(tsf) \text{ for } N_{SPT} > 60 \tag{4}$$

$$Q_s = A_s f_s \tag{5}$$

$$f_s = \frac{N_{SPT}}{34}(tsf) \text{ for } N_{SPT} \leq 53 \tag{6}$$

$$f_s = \frac{N_{SPT}-53}{450} + 1.6(tsf) \text{ for } 53 < N_{SPT} \leq 100. \text{ with condition } f_s \leq 1.7\ tsf \tag{7}$$

where Q_b is the ultimate end bearing (kN), Q_s is ultimate skin resistance (kN), A_b is the base area of the bored pile (m^2), A_s is the cross-sectional area of the bored pile (m^2), f_b is the end bearing per unit area (kPa), and f_s is skin resistance per unit area (kPa).

O'Neill and Reese (1989) Method for Sandy Soil

The ultimate end bearing and skin resistance of bored piles using the O'Neill and Reese (1989) method are obtained by the following equation:

$$f_b = 0.6\, N_{60} \sigma_r \leq 4500\ kPa \tag{8}$$

$$f_s = \beta p_o{}'_{average} \tag{9}$$

$$\beta = 1.5 - 0.245\sqrt{z} \text{ with } 0.25\ \leq \beta \leq 1.2 \tag{10}$$

$$N_{60} \leq 15, \text{ then } \beta = \frac{N_{60}}{15} \times (1.5 - 0.245\sqrt{z}) \tag{11}$$

$$N_{60} = \frac{1}{0.6} \times E_f C_b C_s C_r N_{SPT} \tag{12}$$

where, N_{60} is the average of SPT-N value between the bottom end of the bored pile and 2 d_b below it and no need for overburden correction, σ_r is reference stress = 100 kPa, β is O'Neill and Reese coefficient, $P_o{}'$ is the overburden pressure in the soil layer (kPa), N_{60} is the SPT-N value that is not corrected for overburden and is only corrected by the influence of bor equipment in the field, E_f is hammer efficiency, C_b is a correction to the borehole diameter, C_s is a correction to the SPT sampler tube type, and C_r is a correction to the length of the drill rod.

Reese et al (1977) Method for Clayey Soil

Reese et al. (1977) approach can be used to calculate the skin resistance on clayey soils. According to Hardiyatmo (2018) [10], the method of Reese et al. (1997) using the following formula:

$$f_s = \alpha C_u \tag{13}$$

$$C_u = 7N_{60} \tag{14}$$

where α is the adhesive factor (see Table 2), C_u is undrained cohesion (AASHTO 1998 in Hardiyatmo 2018).

TABLE 2. Correlation between undrained cohesion and adhesive factor

C_u	α
<200	0.55
200-300	0.49
301-400	0.42
401-500	0.38
501-600	0.35
601-700	0.33
701-800	0.32
801-900	0.31
>900	Counted as Rock

The efficiency of Group Pile

The axial bearing of the foundation must consider the efficiency of the group pile to reduce the load working on the pile cap by divided into loads working on a single pile. The efficiency factor is affected by the distance and diameter of the pile. For sandy soils, the converse-Labarre formula can be used by following the equation below:

$$E_g = 1 - \left[\frac{(2-1)m+(m-1)n}{90mn}\right]\theta \tag{15}$$

$$\theta = arc\ tan\left(\frac{D}{s}\right) \tag{16}$$

where E_g is efficiency pile group, m is row count, n is the number of piles in 1 row, D is the diameter of the pile, and s is the distance between piles.

Simplified Procedure for Liquefaction Potential Analysis

The simplified procedure by Idriss and Boulanger (2008) was used for the liquefaction analysis in this study [15]. This method aims to investigate a potential liquefaction occurrence by determining the factor of safety against liquefaction using the following equation:

$$FS_{liq} = CRR/CSR \tag{17}$$

where FS_{liq} is the safety factor, CSR is the cyclic stress ratio, and CRR is the cyclic resistance ratio. CSR was developed by Seed and Idriss (1970) [16] and it was modified by Idriss and Boulanger (2008) using the following equation:

$$CSR = 0.65\frac{a_{max}}{g}\frac{\sigma_{vc}}{\sigma'_{vc}}\frac{1}{MSF}\frac{1}{K_\sigma}r_d \tag{18}$$

where 0.65 coefficient represents a value equal to 65% of peak cyclic stress, a_{max} is peak ground acceleration maximum on the ground surface, σ_{vc} and σ'_{vc} are total and effective vertical stress respectively, *MSF* is the magnitude scaling factor of the moment magnitude 7.5, K_σ is an overburden correction factor, and r_d is a shear stress reduction coefficient that correlates the depth function and magnitude scale. Furthermore, the CRR value can be calculated using the following equation:

$$CRR = exp\left(\frac{(N_1)_{60cs}}{14.1} + \left(\frac{(N_1)_{60cs}}{126}\right)^2 - \left(\frac{(N_1)_{60cs}}{23.6}\right)^3 + \left(\frac{(N_1)_{60cs}}{25.4}\right)^4 - 2.8\right) \tag{19}$$

where $(N_1)_{60cs}$ is the combination of SPT-N value corrected by effective overburden stress (N_1), soil investigation boring equipment (N_{60}), and fines content of soil (N_{cs}).

Liquefaction Induced Soil Bearing Degradation

The soil liquefied is affected by the increase in pore water pressure. The closer the pore water pressure value is to the soil stress value, the lower the effective soil stress, see Equation 20 (Das and Sobhan, 2013) [17]. Researchers Zaw and Yu (2008) [18] used an approach to reduce soil stress due to an increase in pore water pressure on the mat foundation using the following equation:

$$\sigma' = \sigma - u \tag{20}$$

$$Q_u = \frac{1}{2}(1 - \mathrm{r}_u)\gamma_b B N_y \tag{21}$$

where σ' is effective soil stress, σ is soil stress, u is pore water pressure, r_u is pore water pressure ratio, γ_b buoyant unit weight of soil below the foundation, B is the width of the foundation, and N_y is bearing capacity factor.

Excess pore water ratio (r_u) can be calculated by following Equation 21, where Δu is the excessing pore water pressure in kPa and σ'_0 is initial effective stress. The empirical approach for predicting excess pore water ratio was proposed by Yegian and Vitteli (1981) by using the safety factor against liquefaction value [19]. The equation is following Equation 22.

$$r_u = \left(\frac{\Delta u}{\sigma'_0}\right) \tag{22}$$

$$r_u = \frac{2}{\pi}\arcsin\left(\frac{1}{FS_L}\right)^{\frac{1}{2\alpha\beta}} \tag{23}$$

where α and β are constants of 0.7 and 0.19 respectively. Using the same approach as Equation 21, the ultimate bearing capacity of the pile for end bearing and skin resistance can be determined considering the influence of the pore water pressure ratio, so the equation is as follows:

$$Q_b = A_b(1 - r_u)f_b \tag{24}$$

$$Q_s = A_s(1 - r_u)f_s \tag{25}$$

According to the Port and Harbor Research Institute (1997), when there is no effect of r_u so no implication to soil-bearing capacity. When the value of r_u is between 0 and 0.5, the soil bearing capacity begins to reduce but remains stable. When the value of r_u reaches 1.0 it will quickly become 1.0 or liquefaction occurs then affecting the losses of soil-bearing capacity [20]. Thus, Equations 24 and 25 can explain the relationship between r_u and loss of soil bearing capacity.

Bridge Modeling in MIDAS GTS NX

MIDAS GTS NX is one of MIDAS's software that can model piles with 3D numerical simulation. MIDAS GTS NX considers the pile spring and the reaction of the soil layer by modeling them in a 3D numerical simulation so that the soil reaction to the load applied to the pile is known. MIDAS GTS NX uses the interface wizard interaction to model the stiffness of the pile interface using the following formula:

$$K_n = \frac{E_{oed,i}}{(L \times tv)} \tag{26}$$

$$K_t = \frac{G_i}{(L \times tv)} \tag{27}$$

$$E_{oed,i} = \frac{2 \times Gi \times (1 - vi)}{(1 - 2 \times vi)} \tag{28}$$

$$G_i = R \times G_{soil} \tag{29}$$

$$G_{soil} = \frac{E}{2 \times (1 + v_{soil})} \tag{30}$$

where K_n is interface normal stiffness, K_t is interface shear stiffness, $E_{oed,i}$ is interface drained soil young's modulus, L is the length of pile interaction, tv is the virtual thickness (generally has a value between 0.01-0.1), G_i is interface shear modulus, vi is interface Poisson's ratio = 0.45, G_{soil} is soil shear modulus, R is strength reduction factor, E is Young's modulus, and v_{soil} is soil Poisson's ratio. In general, the strength reduction factor for structural members and contiguous ground properties are as follows; Sand/Steel = 0.6-0.7, Clay/Steel = 0.5, Sand/Concrete = 1.0-0.8, and Clay/Concrete = 1.0-0.7. Another researcher, Jeongsik (2018), stated that for sandy soil with liquefied state, 3-dimensional numerical analysis by finite element analysis was applied to the model pile inserted into the soft clay soil [21]. In this model, the cohesion value used during the liquefaction state is 25-30 kPa. The summary of soil properties input in static and liquefaction states is shown in Table 3 and Table 4 below:

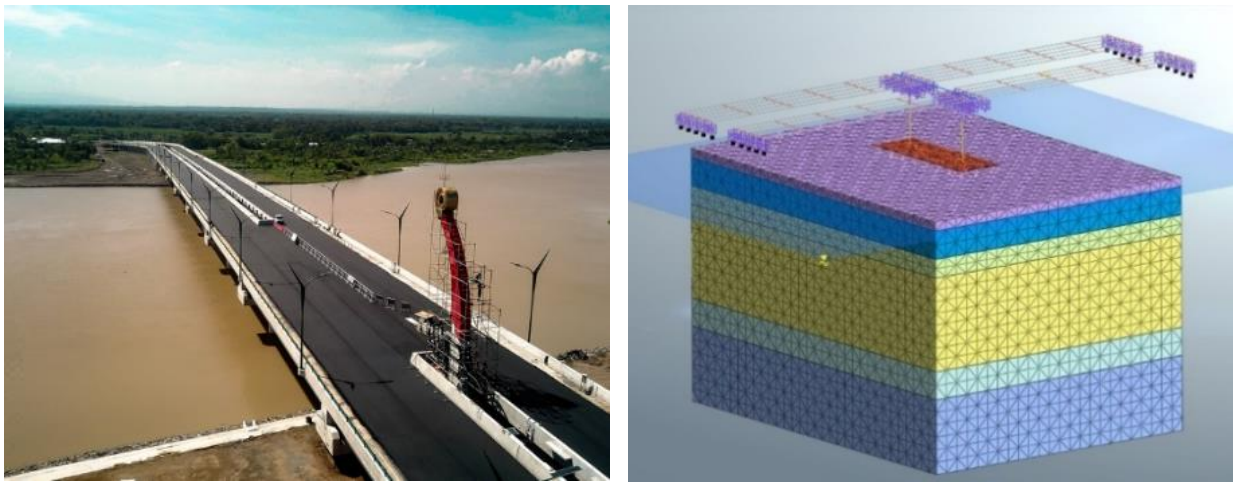

(a) (b)

FIGURE 3. (a) Kretek 2 Bridge bird view [22] (b) Modeling in MIDAS GTS NX

TABLE 3. Soil properties input in the static state

Depth (m)	γ_{bulk} (kN/m^3)	γ_{sat} (kN/m^3)	ϕ (°)	E (kN/m^2)	μ	G_{soil} (kN/m^2)	E_{oed} (kN/m^2)	K_n (kN/m^2)	K_t (kN/m^3)
0.0-1.5	16.84	19.05	34	19800.00	0.35	7342.04	64609.91	430732.72	48946.90
1.5-9.0	18.33	20.54	38	49550.00	0.36	18173.15	159923.71	1066158.09	121154.33
9.0-24.0	20.00	22.21	41	83033.33	0.38	30084.18	264740.76	1764938.43	200561.18
24.0-28.5	18.80	21.01	39	59000.00	0.37	21564.33	189766.08	1265107.21	143762.18
28.5-34.5	21.33	23.54	42	109666.67	0.39	39354.07	346315.79	2308771.93	262360.45

TABLE 4. Soil properties input in the liquefaction state

Depth (m)	γ_{bulk} (kN/m^3)	γ_{sat} (kN/m^3)	ϕ (°)	E (kN/m^2)	μ	G_{soil} (kN/m^2)	E_{oed} (kN/m^2)	K_n (kN/m^2)	K_t (kN/m^3)
0.0-6.0	15.00	18.00	0	500	0.45	172.41	1517.24	10114.94	1149.43
6.0-9.0	18.73	20.94	39	57541.67	0.39	39354.07	185174.24	1234494.91	140283.51
9.0-24.0	20.00	22.21	41	83033.33	0.38	30084.18	264740.76	1764938.43	200561.18
24.0-28.5	18.80	21.01	39	59000.00	0.37	21564.33	189766.08	1265107.21	143762.18
28.5-34.5	21.33	23.54	42	109666.67	0.39	39354.07	346315.79	2308771.93	262360.45

Pile Testing

According to Ariyanto and Untung (2013), the pile driving analysis (PDA) test is based on data analysis of recorded shaft vibrations that occur when the hammer strikes the pile [23]. Strain and shaft acceleration due to ram tool impact was measured using a strain transducer and an accelerometer. The results of the strain and acceleration measurements are required to estimate the bearing capacity of the pile using the one-dimensional wave theory. Another analysis is

the CAPWAP analysis which is performed along with the PDA test, which is one of the Signal Matching Analysis (SMA) methods. From the CAPWAP analysis, we can establish the data obtained from the PDA test in more detail, with additional information in the form of end bearing and skin resistance of single-pile foundation and static simulation load test. The results of the PDA test on the Kretek 2 Bridge are shown in Table 5 below:

TABLE 5. Ultimate bearing capacity of Piles for PDA and CAPWAP result

Abutment/ Pier	PDA (kN)	Ultimate bearing capacity (kN)		
		Total	Skin resistance	End Bearing
P1	5111.01	8338.50	6768.90	1569.60
P2	6690.42	8829.98	7554.68	1275.30
P4	8750.52	10791.00	9025.20	1765.80
P7	5856.57	8790.74	7043.58	1748.14
P8	8691.66	9810.98	8339.48	1471.50
ABT2	9368.55	9809.02	7847.02	1962.00

According to Likins (2004), pile driving analysis (PDA) tests in the field using a safety factor value = 2.0 to compare with load design [24].

Research Diagram

Research data includes SPT-N test data, soil properties, bridge design, bridge load, pile driving analysis test, liquefaction potential with safety factor value, and excess pore water pore ratio. This study aims to determine the bearing capacity under static and liquefaction conditions using the empirical approach and 3D numerical simulation. The stages of the investigation are illustrated in Figure 4 below:

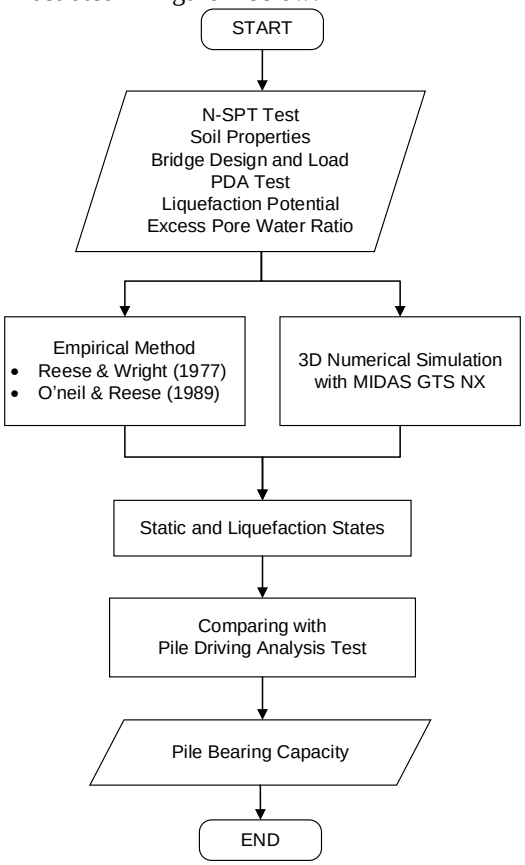

FIGURE 4. Flow diagram of research

RESULT AND DISCUSSION

Soil Stratigraphy and Liquefaction Potential

The Opak River estuary is generally composed of sandy soil with various densities, but mainly in a dense sand category. In a previous study by Zakariya et al (2022) [25], The soil investigation shows the soil in loose-medium-sand at BH-1, BH-2, BH-3, BH-5, BH-6, BH-7, and BH-8, in 1.5-6m depth (see Figure 5 and 6a). Several boreholes in BH-1, BH-2, and BH-07 has clayey soil layer with various depth of 27-39 m. However, liquified soil only occurs maximum depth of 20 m. The simplified procedure showed various CSR values from 0.346 to 0.603 and various CRR values from 0.168 to 2.0. The thickness at point BH-6 has a liquefied layer at depths of 0-1.5 m and 4.5-6.0 m (see Figure 6b). The thickness of a liquefiable layer is crucial as it will become a reference in later soil and foundation modeling.

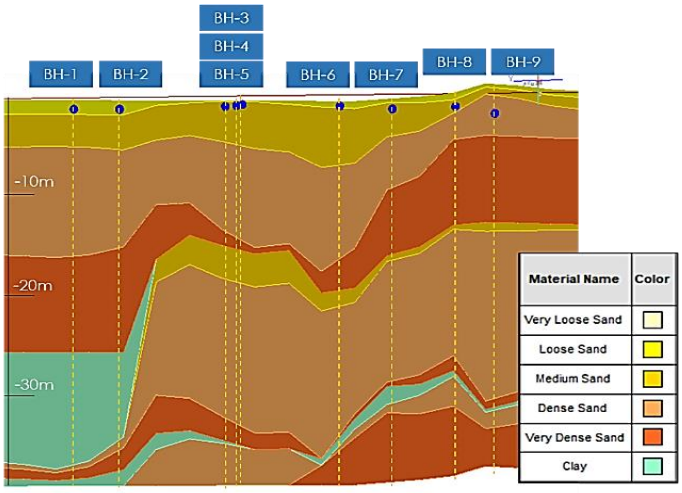

FIGURE 5. Soil stratigraphy

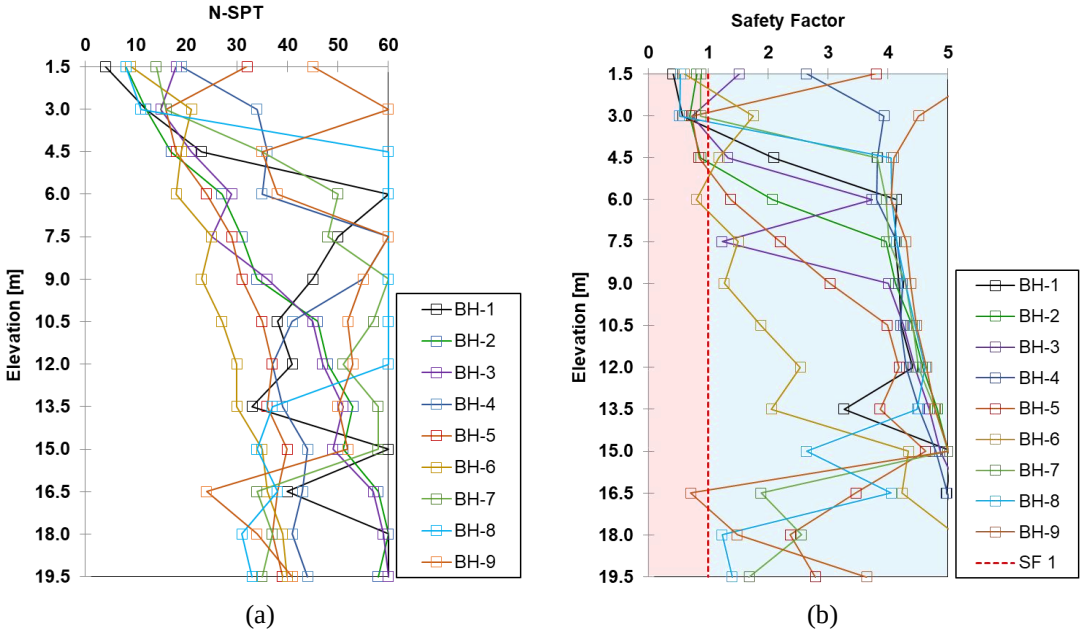

FIGURE 6. (a) SPT-N value of each borehole (b) Safety factor against liquefaction

Empirical Approach Output

Empirical calculations result in two ultimate pile capacities: tip resistance and skin resistance. The end bearing value is different in each soil depth layer, and the value used is the mean value of the layer at the tip of the bored pile. Skin resistance, however, shows a graph that increases with soil depth, and the value used is the cumulative value from the ground surface to the tip of the bored pile. The calculation results using Reese and Wright (1977) for sandy soils and Reese et al (1977) for clayey soils gave different values. This difference results from the soil types in each layer, the number of piles, and the length of piles used for each pier/abutment (see Figures 7 to 9). This value has yet to be multiplied by the safety factor. As a result, the minimum values are 2809.98 kN, 11455.99 kN, and 13615.40 kN for end bearing, skin resistance, and total ultimate bearing capacity respectively for Pier 6 and Pier 7, respectively. The maximum values are 3141.59 kN, 14746.92 kN, and 17237.94 kN for end bearing, skin resistance, and total ultimate bearing capacity respectively for Pier 8.

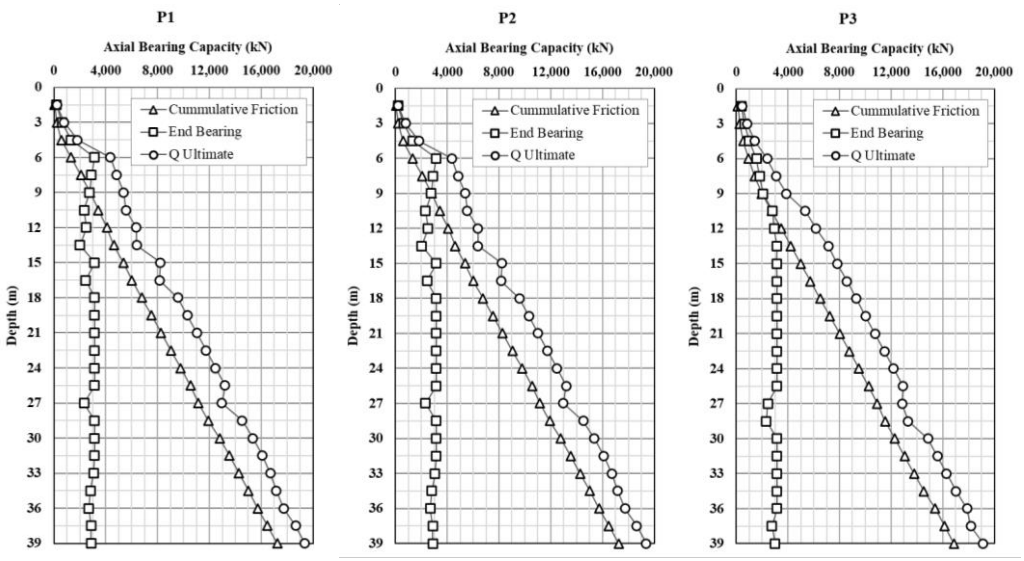

FIGURE 7. Bearing capacity using Reese and Wright (1977) on Pier 1, 2, and 3

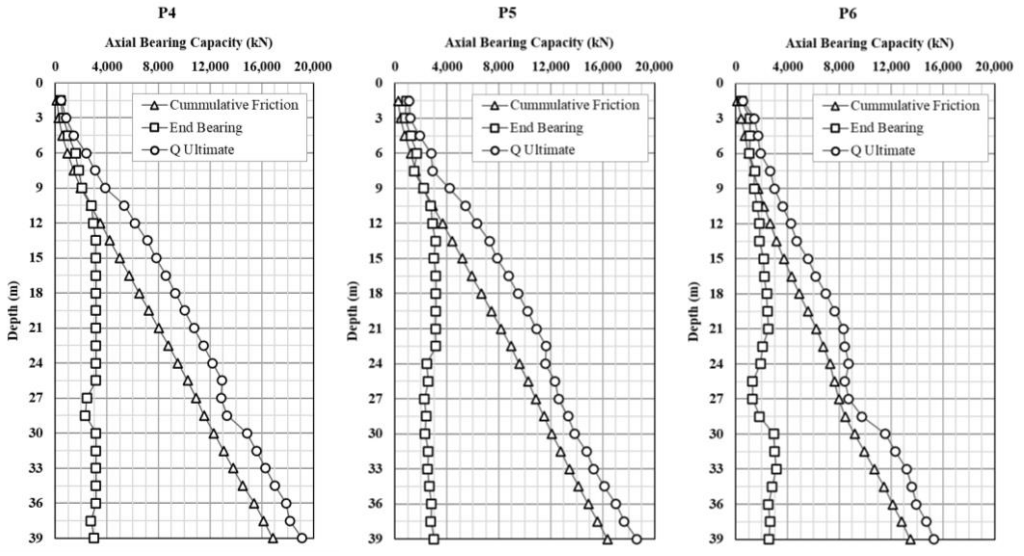

FIGURE 8. Bearing capacity using Reese and Wright (1977) on Pier 4, 5, and 6

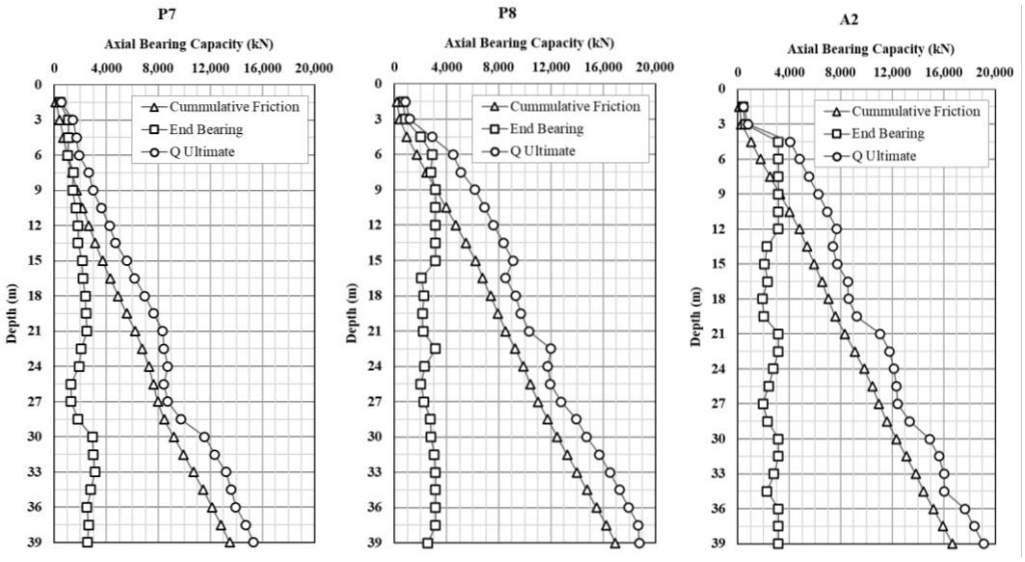

FIGURE 9. Bearing capacity using Reese and Wright (1977) on Pier 7 and 8, and Abutment A2

Different values were also obtained in the calculation results according to O'Neill and Reese (1989) for sandy soil and Reese et al (1977) for clayey soils (see Figures 10 to 12). The minimum values are 2310.00 kN, 12772.88 kN, and 14488.88 kN for end bearing, skin resistance, and total ultimate bearing capacity at Pier 5, respectively. The maximum values are 2860.00 kN, 14613.86 kN, and 16823.29 kN for end bearing, skin resistance, and total ultimate bearing capacity at Pier 8. The value of the axial bearing capacity determined using the method of O'Neill and Reese (1989) is slightly smaller than that according to Reese and Wright (1977). This result shows that O'Neill and Reese's (1989) method is relatively more conservative.

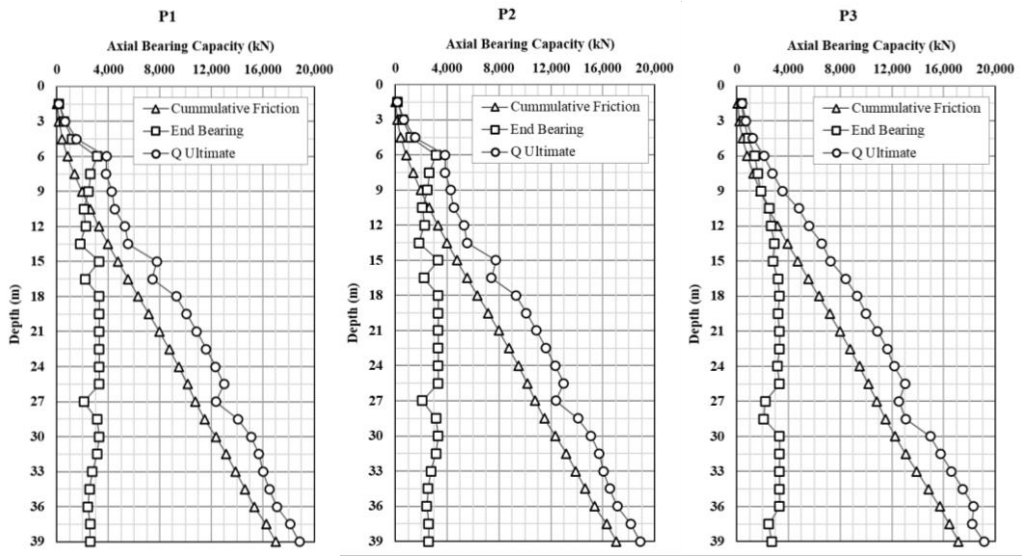

FIGURE 10. Bearing capacity using O'Neill and Reese (1989) on Pier 1, 2, and 3

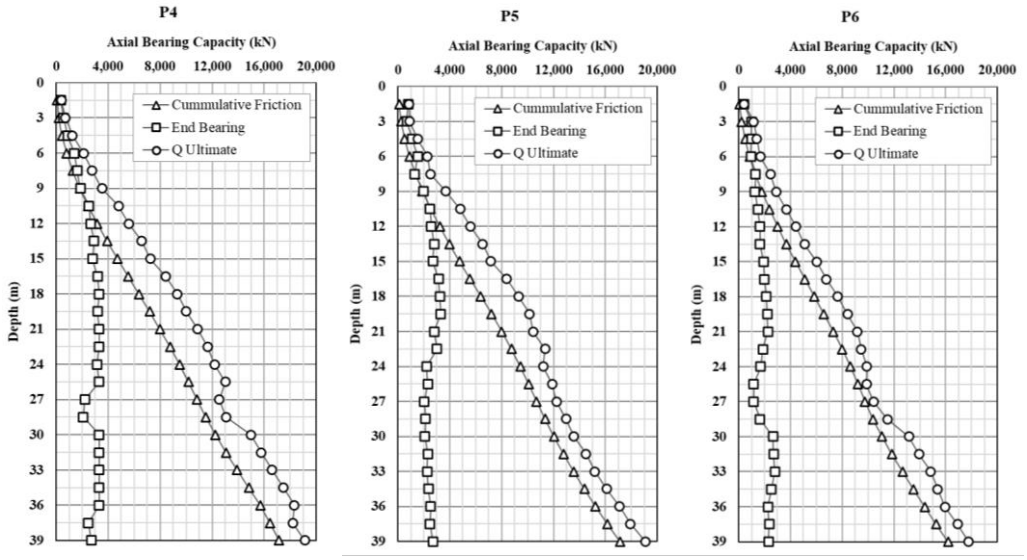

FIGURE 11. Bearing capacity using O'Neill and Reese (1989) on Pier 4, 5, and 6

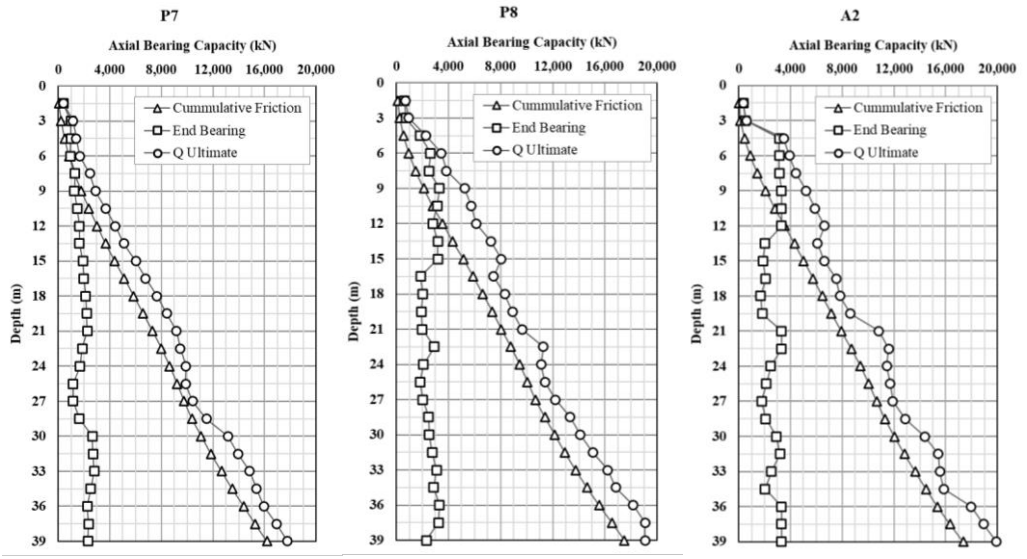

FIGURE 12. Bearing capacity using O'Neill and Reese (1989) on Pier 7 and 8, and Abutment A2

Under the liquefaction state using Formulas 24 and 25, skin resistance reduction occurred. It is because liquefaction conditions predominantly occur only in the top soil layer (0–6 m), while the length of the pile reaches 32–34 m, so liquefaction does not affect the end bearing capacity. The decrease in the axial bearing capacity shows a relatively similar and constant value for both methods (Reese and Wright and O'Neill and Reese). The decrease occurred between 2.88-8.16% for the Reese and Wright (1977) method and 2.63-7.23% for O'Neill and Reese (1989). The lowest percent decrease occurred in P1 and P2, while the largest percent decrease occurred in P6 and P7. This variation in value occurs due to differences in the thickness of the liquefied soil layer in each pier/abutment. The thicker the liquefied layer, the greater the value of the decrease that occurs.

The value of the axial load capacity reduction according to the empirical method is shown in the following Table 6 below:

TABLE 6. Axial bearing capacity losses using empirical methods

Abt/ Pier	Reese and Wright (1977)			O'neil and Reese (1989)		
	Q Ultimate (kN)		Axial bearing losses (%)	Q Ultimate (kN)		Axial bearing losses (%)
	Static State	Liquefaction State		Static State	Liquefaction State	
P1	15707.13	15255.01	2.88	16090.23	15667.26	2.63
P2	15713.69	15261.39	2.88	16090.23	15667.26	2.63
P3	15765.43	14982.64	4.97	15582.64	14875.87	4.54
P4	15765.43	14982.64	4.97	15582.64	14875.87	4.54
P5	14488.88	13836.82	4.50	14753.64	14114.41	4.33
P6	15385.32	14129.50	8.16	13615.40	12630.84	7.23
P7	15385.32	14129.50	8.16	13615.40	12630.84	7.23
P8	16823.29	16054.69	4.57	17237.94	16472.81	4.44
A2	15846.73	14979.97	5.47	16045.55	15271.86	4.82

Empirical vs. PDA Test

The empirically determined value in the static state as the design bearing capacity must be checked using pile tests. In Table 5, the values of end bearing, skin resistance, and total axial ultimate bearing were previously known by PDA test. This result can also compare the design load acting on each pile in Table 1, but it must first be multiplied by the efficiency of the pile group and only then divided by the number of piles. The PDA test value (with a safety factor of 2.0) compared to the value of the design capacity or bearing capacity nominal with a safety factor of 3.0 using empirical calculations according to the method of Reese and Wright (1977) showed values that at P3, P4, P5, P6, and P7 almost the same. Meanwhile, the PDA test value is below the design capacity value at P1, P2, P8, and A2 (see Figure 13). However, the PDA value is still above the design load value for each abutment/pier such that the embedded bored pile is in its position sufficiently capable of supporting the loads applied to it.

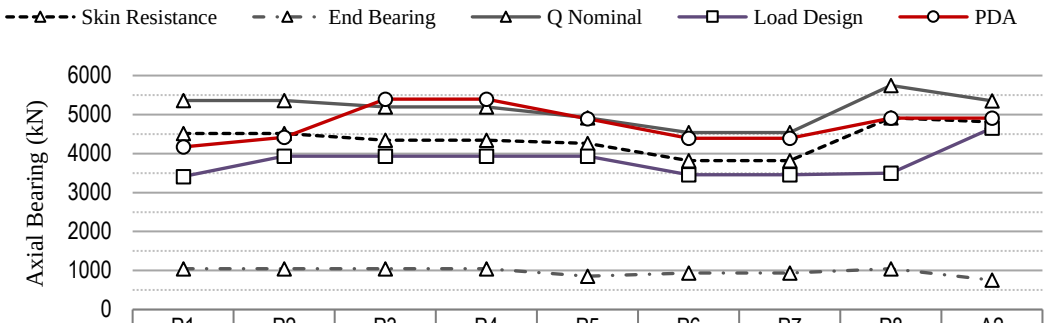

	P1	P2	P3	P4	P5	P6	P7	P8	A2
Skin Resistance	4514,21	4514,21	4345,02	4345,02	4260,67	3818,66	3818,66	4915,64	4811,97
End Bearing	1047,20	1047,20	1047,20	1047,20	855,21	936,66	936,66	1047,20	753,40
Q Nominal	5363,41	5363,41	5194,21	5194,21	4917,88	4538,47	4538,47	5745,98	5348,52
Load Design	3410,74	3928,74	3928,74	3928,74	3928,74	3456,02	3456,02	3494,63	4653,60
PDA	4169,25	4414,99	5395,50	5395,50	4895,44	4395,37	4395,37	4905,49	4904,51

FIGURE 13. Design pile bearing in the static state using Reese and Wright (1977)

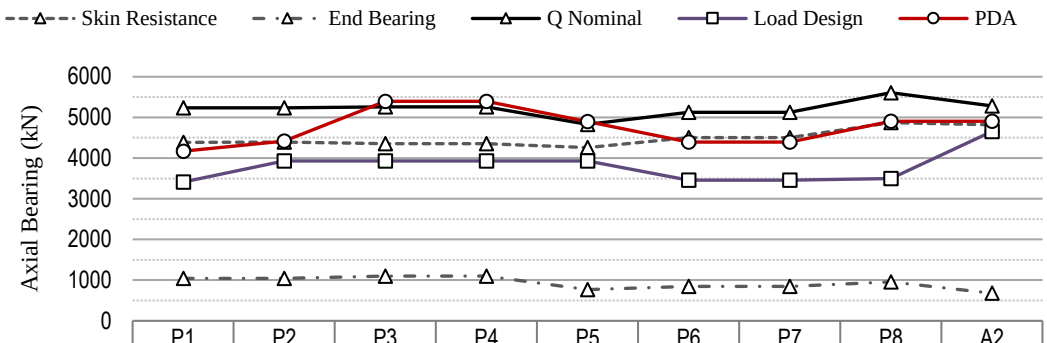

	P1	P2	P3	P4	P5	P6	P7	P8	A2
Skin Resistance	4389,13	4390,90	4353,14	4353,14	4257,63	4501,97	4501,97	4871,29	4820,77
End Bearing	1044,58	1045,00	1100,00	1100,00	770,00	843,33	843,33	953,33	678,33
Q Nominal	5235,71	5237,90	5255,14	5255,14	4829,63	5128,44	5128,44	5607,76	5282,24
Load Design	3410,74	3928,74	3928,74	3928,74	3928,74	3456,02	3456,02	3494,63	4653,60
PDA	4169,25	4414,99	5395,50	5395,50	4895,44	4395,37	4395,37	4905,49	4904,51

FIGURE 14. Design pile bearing in the static state using O'Neill and Reese (1989)

Meanwhile, the empirical calculation by O'Neill and Reese (1989) also shows a relatively consistent value with the previous method's calculation. The PDA test value results with the pile's design capacity are almost identical at P3, P4, and P5. Meanwhile, the PDA test value is below the design capacity value at P1, P2, P6, P7, P8, and A2 (see Figure 14). While some design capacity values are below the PDA test, it is still above the load design value for each abutment/pier for the bored pile embedded in position to have sufficient capacity to carry the working load.

Under liquefaction conditions, both methods, according to Reese and Wright (1977) and O'Neill and Reese (1989), still performed well in supporting the design loads acting on each pile (see Figures 15 and 16). Thus, the bored pile foundation on each pier/abutment can support the design load under static and liquefaction states, although there is a decrease in bearing capacity is less than 8.16% and 7.23% for Reese and Wright (1977) and O'Neill and Reese (1989) method respectively.

The use of the safety factor in the empirical method of 3.0 must be considered again in the numerical method with the pile test due to comparing the pile bearing capacity design with the actual condition

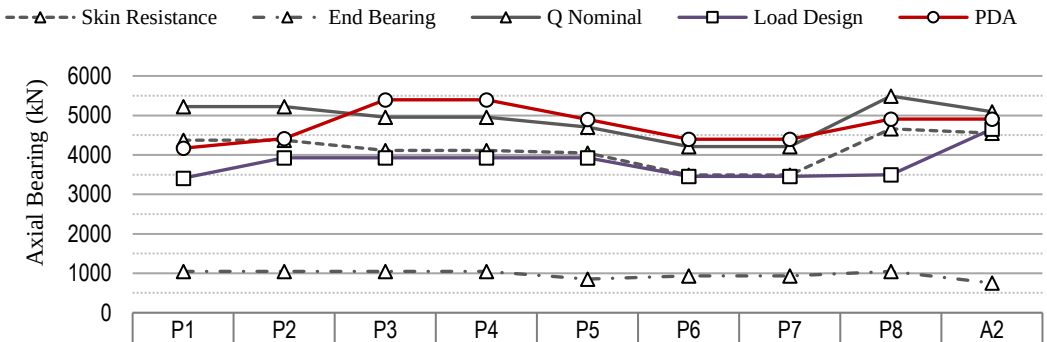

	P1	P2	P3	P4	P5	P6	P7	P8	A2
Skin Resistance	4373,22	4373,22	4109,43	4109,43	4047,59	3490,48	3490,48	4660,60	4554,08
End Bearing	1047,20	1047,20	1047,20	1047,20	855,21	936,66	936,66	1047,20	753,40
Q Nominal	5222,42	5222,42	4958,62	4958,62	4704,80	4210,28	4210,28	5490,94	5090,62
Load Design	3410,74	3928,74	3928,74	3928,74	3928,74	3456,02	3456,02	3494,63	4653,60
PDA	4169,25	4414,99	5395,50	5395,50	4895,44	4395,37	4395,37	4905,49	4904,51

FIGURE 15. Design pile bearing in liquefaction state using Reese and Wright (1977)

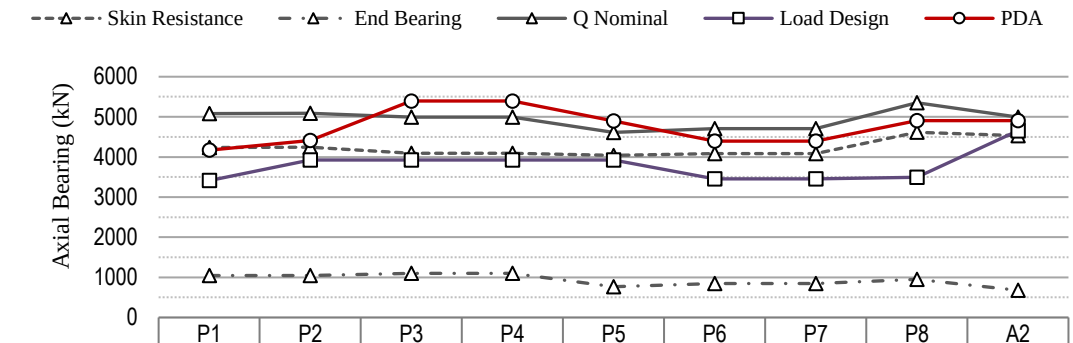

	P1	P2	P3	P4	P5	P6	P7	P8	A2
Skin Resistance	4238,42	4240,13	4092,21	4092,21	4040,27	4083,36	4083,36	4615,09	4531,85
End Bearing	1044,58	1045,00	1100,00	1100,00	770,00	843,33	843,33	953,33	678,33
Q Nominal	5085,00	5087,13	4994,21	4994,21	4612,27	4709,83	4709,83	5351,56	4993,32
Load Design	3410,74	3928,74	3928,74	3928,74	3928,74	3456,02	3456,02	3494,63	4653,60
PDA	4169,25	4414,99	5395,50	5395,50	4895,44	4395,37	4395,37	4905,49	4904,51

FIGURE 16. Design pile bearing in liquefaction state using O'Neill and Reese (1989)

3D Numerical Output

Bridge modeling to compare the empirical method on Pier 7 with considering Pier 7 is the highest value decreasing for axial bearing capacity in liquefaction state. Considering the liquefaction layer at a depth of 0–6.0 m is assumed as the worst-case scenario for this model on Pier 7. One of the advantages of using MIDAS GTS NX is that it can generate an axial bearing capacity based on the option of pile force as skin resistance (kN/m) and pile tip as end bearing (kN) (see Figures 17a and 17b). The resulting axial bearing capacity is a reaction of load applied to the pile and then transferred to each layer of soil. Midas GTS NX also shows solid strain e-equivalent in each soil layer (see Figure 18), indicated in green to red colors with *higher* solid strain value as a liquefiable layer.

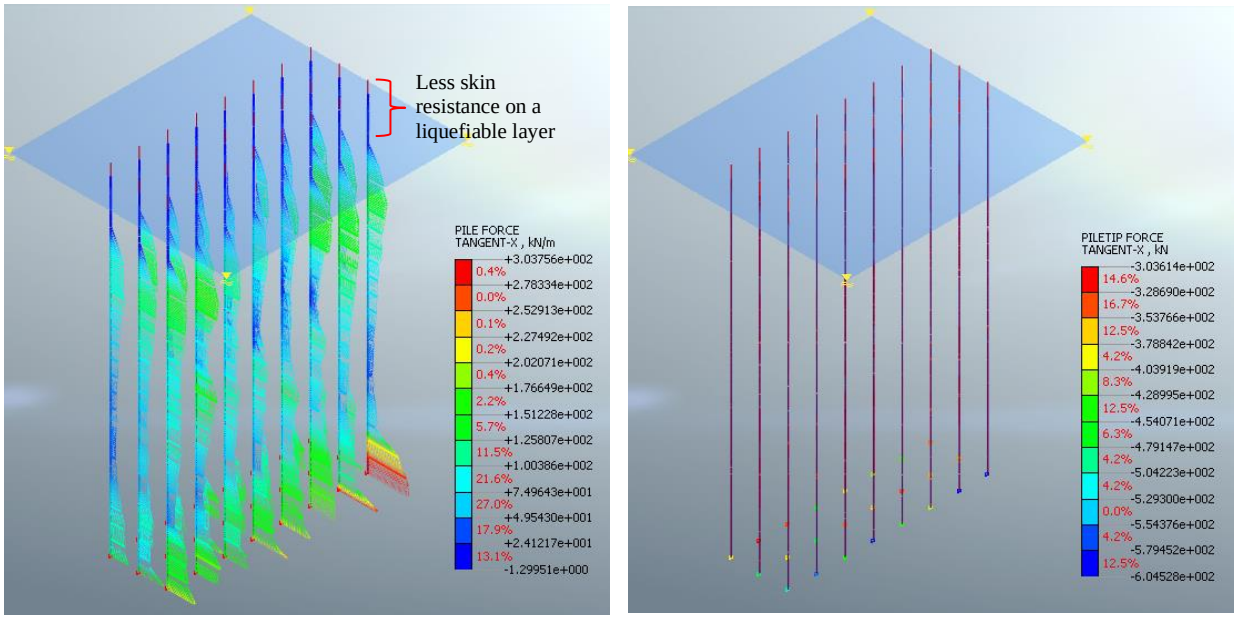

(a) (b)

FIGURE 17. MIDAS GTS NX output (a) Pile force (b) Pile tip force

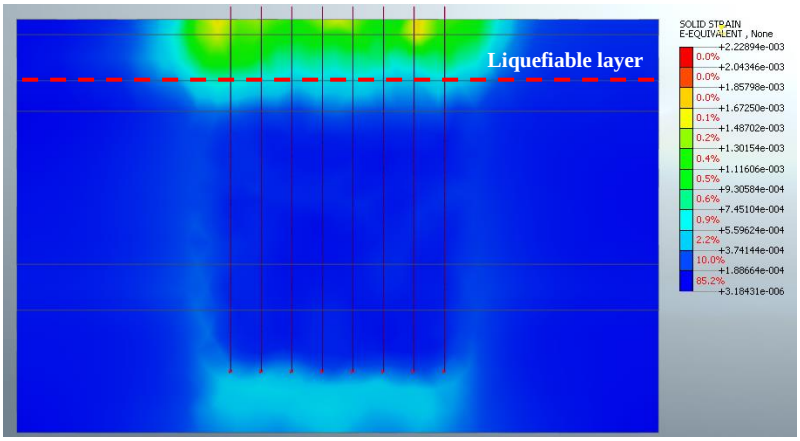

FIGURE 18. MIDAS GTS NX output for solid strain e-equivalent

Empirical vs. 3D Numerical

Midas GTS NX can use for modeling soil layers with 3D numerical simulations and piles as a soil structure interaction so that the value of the axial bearing capacity (skin resistance and end bearing) shows up. The results of the bearing capacity examination show that the Kretek 2 bridge foundation is sufficient to carry the axial load in the static and liquefaction state. Considering maximum axial load design and pile driving analysis (PDA) tests show the axial load carrying capacity of 3660.48 kN and 3632.56 kN for static and liquefaction states, respectively. This value is slightly above the design load = 3456.02 kN and below the PDA test value = 4480.50 kN, as shown in Figure 19. The value of axial bearing capacity in the static and liquefaction state indicates that the value tends not to change significantly. MIDAS GTS NX can estimate the axial bearing capacity under static or liquefaction conditions. However, the resulting value is close to the design load value, so using MIDAS GTS NX is more conservative for this study. The empirical method is easier and faster to estimate the pile capacity compared to modeling with 3D numerical simulation. However, the empirical method needs careful consideration of the bridge design's safety factor value usage.

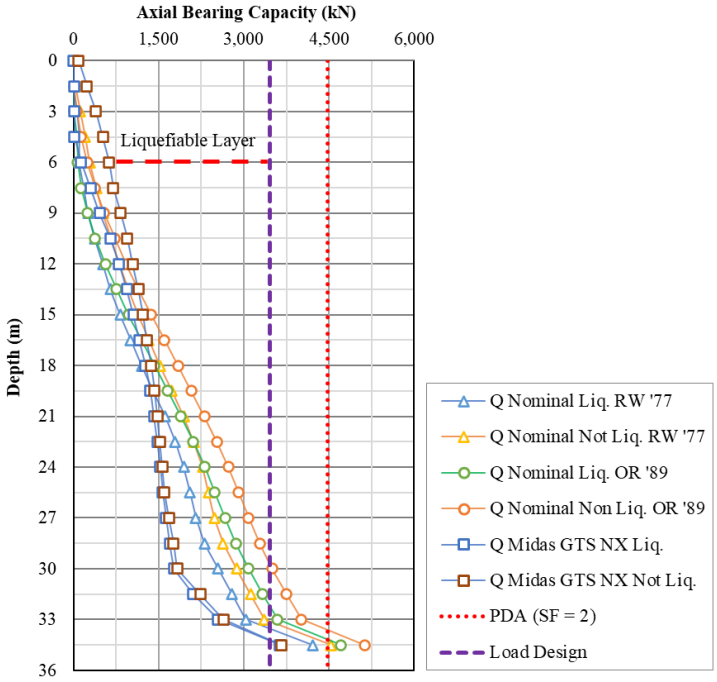

FIGURE 19. Comparison of axial bearing capacity from various methods on Pier 7

For further research, the bridge can be modeled by time history dynamic analysis and particular sand materials such as UBCSand so that the model is nearly close to the actual condition. A static loading test must be carried out for the field test to ensure the axial bearing capacity for actual conditions.

CONCLUSION

The results of this study show that:

1. Based on previous investigations, liquefaction potential exists at various depths, most of which occur in the top layer from 0-6m.
2. PDA value is still above the design load value for each abutment/pier, so the bored pile can sufficiently support the loads applied.
3. Under the liquefaction state, the ultimate bearing capacity decreased. The decrease between 2.88-8.16% for the Reese and Wright (1977) method and 2.63-7.23% for O'Neill and Reese (1989). The lowest percent decrease occurred in P1 and P2, while the largest percent decrease occurred in P6 and P7. Nevertheless, the total bearing capacity in static and liquefaction conditions is 4210.28 kN and 4709.83, higher than the design load of 3456.02 kN with a factor of safety of 3.0.
4. MIDAS GTS NX result, both in static and liquefaction states, is slightly above the design load and below the PDA test. There was no significant decrease in the total bearing capacity, and it was still above the design load (3632.56>3456.02 kN). This method's result is more conservative than the empirical method.
5. The empirical method is easier and faster with manual calculation to estimate the pile capacity compared to modeling with 3D numerical simulation. However, the empirical method needs careful consideration of the bridge design's safety factor value usage.
6. The bearing capacity of the Kretek 2 bridge bored pile foundation embedded in the field can still accommodate static and liquefaction conditions.

ACKNOWLEDGMENTS

The authors give enormous gratitude to the Unit Work of National Road Implementation (PJN) Yogyakarta Special Region Province Territory, National Road Implementation Agency (BBPJN) of Central Java – Yogyakarta Special Region for soil investigation data support.

REFERENCES

[1] P. M. Byrne, E. Naesgaard, and M. Seid-Karbasi, "Analysis and Design of Earth Structures to Resist Seismic Soil Liquecation," 2006.

[2] S. R. Dash, S. Bhattacharya, and A. Blakeborough, "Bending-buckling interaction as a failure mechanism of piles in liquefiable soils," *Soil Dyn. Earthq. Eng.*, vol. 30, no. 1–2, pp. 32–39, 2010, doi: 10.1016/j.soildyn.2009.08.002.

[3] Direktorat Jenderal Bina Marga, *Panduan Praktis Perencanaan Teknis Jembatan*, 02/M/BM/20. Jakarta: Direktorat Jenderal Bina Marga, 2021.

[4] G. Madabhushi, J. Knappett, and S. Haigh, "Design of pile foundations in liquefiable soils," *Design of Pile Foundations in Liquefiable Soils*. pp. 1–217, 2009, doi: 10.1142/P628.

[5] Badan Geologi, *Atlas Zona Kerentanan Likuefaksi Indonesia*. Bandung: Kementerian Energi Sumber Daya Mineral, 2019.

[6] Y. Muntafi, N. Nojima, and A. U. Jamal, "Damage Probability Assessment of Hospital Buildings in Yogyakarta, Indonesia as Essential Facility due to an Earthquake Scenario," *J. Civ. Eng. Forum*, vol. 6, no. 3, p. 225, 2020, doi: 10.22146/jcef.53387.

[7] E. K. Sari, "Perancangan Fondasi Tiang Bor pada Jembatan Kretek 2 Bantul, Yogyakarta," Universitas Gadjah Mada, 2017.

[8] Badan Standardisasi Nasional Indonesia, *SNI 1725:2016 Pembebanan untuk Jembatan*, vol. 1725. 2016.

[9] A. Zakariya, A. Rifa'i, and S. Ismanti, "Seismic load reduction on the bridge over liquefaction vulnerability zone by lead rubber bearing," *7th International Conference on Sustainable Built Environment* (ICSBE), Yogyakarta: Universitas Islam Indonesia, 2022.

[10] H. C. Hardiyatmo, *Analisis dan Perancangan Fondasi II*, 4th ed. Yogyakarta: Gadjah Mada University Press,

2018.
[11] G. G. Meyerhof, “Bearing Capacity and Settlement of Pile Foundations,” *ASCE J Geotech Eng Div*, vol. 102, pp. 197–228, 1976.
[12] L. C. Reese and S. J. Wright, “Drilled Shaft Manual, Volume I, Construction Procedures and Design for Axial Loading,” Washington, DC, 1977.
[13] M. W. O’Neill and L. C. Reese, “New Design Method for Drilled Shaft From Common Soil and Rock Tests,” in *Foundation Engineering - Current Principles and Practices*, 1989, pp. 1026–1039.
[14] L. C. Reese, F. T. Touma, and M. W. O’neill, “Behaviour of Drilled Piers Under Axial Loading,” *J. Geotech. Geoenvironmental Eng.*, vol. 102, pp. 493–510, 1977.
[15] I. M. Idriss and R. W. Boulanger, “Soil Liquefaction During Earthquakes,” *Mach. Prod. Eng.*, vol. 160, no. Earthquake Engineering Research Institute, p. 43, 2008, doi: 10.1177/136218079700300202.
[16] H. B. Seed and I. M. Idriss, *A Simplified Procedure for Evaluating Soil Liquefaction Potential*, no. November. California: University of California, 1970.
[17] B. M. Das and K. Sobhan, *Principles of Geotechnical Engineering*, Ninth., vol. 53, no. 9. Boston: Cengage Learning, 2013.
[18] M. T. Zaw and K. T. Yu, “Stability Analysis of A Tall Building with Mat Foundation over Sandy Soil with Soil-Structure Interaction Approach,” in *2nd International Conference on Built Environment in Developing Countries 2008*, 2008, no. Icbedc, pp. 362–391.
[19] M. K. Yegian and B. M. Vitelli, “Analysis for Liquefaction : Empirical Approach,” *Int. Conf. Recent Adv. Geotech. Earthq. Eng. Soil Dyn.*, no. Int. Conf. Recent Adv. Geotech. Earthq. Eng. Soil Dyn., pp. 1–6, 1981.
[20] Port and Harbour Research Institute, *Handbook on liquefaction remediation of reclaimed land*. Rotterdam: A.A. Balkema, 1997.
[21] P. Jeongsik, “Nonlinear 3-Dimensional Analysis of Dynamic P-y Curve in Sand,” Yonsei University, 2018.
[22] A. Zakariya, “Laporan Kegiatan Magang : LOT 3 – Pembangunan Jembatan Kretek 2,” Sleman, 2022.
[23] D. D. Ariyanto and D. Untung, “Studi daya dukung tiang pancang tunggal dengan beberapa metode analisa,” *J. Tek. POMITS*, vol. 1, no. 1, pp. 1–5, 2013.
[24] G. Likins, “Pile Testing - Selection and Economy of Safety Factors,” vol. 40743, no. July 2004, pp. 239–252, 2004, doi: 10.1061/40743(142)14.
[25] A. Zakariya, A. Rifa’i, and S. Ismanti, “Ground Motion and Liquefaction Study at Opak River Estuary Bantul,” *5th International Conference on Eartquake Engineering and Disaster Mitigation* (ICEEDM), Yogyakata: Universitas Gadjah Mada, 2022.